

# OPERATIONAL AND DIAGNOSTIC EVALUATIONS OF THE OZONE FORECASTS BY THE ETA-CMAQ MODEL SUITE DURING THE 2002 NEW ENGLAND AIR QUALITY STUDY (NEAQS)

Shaocai Yu<sup>+\$\*</sup>, Rohit Mathur<sup>+</sup>, Daiwen Kang<sup>+\$</sup>, Kenneth Schere<sup>+</sup>,  
Brian Eder<sup>+</sup>, and Jonathan Pleim<sup>+</sup>

Atmospheric Sciences Modeling Division, Air Resources Laboratory,  
National Oceanic and Atmospheric Administration, RTP, NC 27711

<sup>+</sup>On assignment to National Exposure Research Laboratory,  
U.S. Environmental Protection Agency, Research Triangle Park, NC 27711

<sup>\$</sup>On assignment from Science and Technology Corporation,  
10 Basil Sawyer Drive, Hampton, VA 23666-1393

e-mail: [yu.shaocai@epa.gov](mailto:yu.shaocai@epa.gov)

Voice (919) 541-0362 Fax (919) 541-1379

## 1. INTRODUCTION

Ozone (O<sub>3</sub>), a secondary pollutant, is created in part by emissions from anthropogenic and biogenic sources. It is necessary for local air quality agencies to accurately forecast ozone concentrations to warn the public of unhealthy air and to encourage people to voluntarily reduce emissions-producing activities.

## 2.0 DESCRIPTION OF THE ETA-CMAQ FORECAST MODEL SUITE AND OBSERVATIONAL DATABASE

The Eta-CMAQ air quality forecasting system is based on the National Centers for Environmental Prediction's (NCEP's) Eta model (Rogers et al., 1996) and the U.S. EPA's CMAQ Modeling System (Byun and Ching 1999). In this study, the modeling system is deployed over the domain of the northeast U.S. (Figure 1). The horizontal domain has a grid spacing of 12 km. 22 layers of variable thickness set on a sigma-type coordinate are used to resolve the vertical extent from the surface to 100 hPa. The primary Eta-CMAQ model forecast for next-day's surface-layer O<sub>3</sub> is based on the current day's 12 UTC Eta cycle. The target forecast period is local midnight through local midnight (04 UTC to 03 UTC for the Northeast U.S.).

The hourly O<sub>3</sub> data at 342 sites in the northeast U.S. are available from the U.S. EPA's

AQS network (Figure 1). The four Atmospheric Investigation, Regional Modeling, Analysis, and Prediction (AIRMAP) sites and Harvard Forest (HF) provided continuous measurements of O<sub>3</sub> and related photochemical species as well as meteorological parameters during the NEAQS 2002 (see Figure 1). The four AIRMAP sites include Castle Springs (CS), Isle of Schoals (IS), Mount Washington Observatory (MWO), and Thompson Farm (TF) sites. O<sub>3</sub> Lidar vertical profiles obtained on the NOAA ship Ronald H. Brown during the NEAQS 2002 were used to assess the vertical concentrations. The model performance from August 6 to August 17, 2002, based on the 12 UTC run for the target forecast period is examined in this study.

## 3.0 RESULTS AND DISCUSSIONS

### 3.1 Operational evaluation over the NE U.S. domain at the AQS sites

For the discrete evaluation, we calculated summary and regression statistics along with two measures of bias: the Mean Bias (MB) and the Normalized Mean Bias (NMB); and two measures of error: the Root Mean Square Error (RMSE) and Normalized Mean Error (NME) (see Table 1). The model reproduced 53.3, 88.6 and 83.5% of the observed hourly, maximum 1-hr and maximum 8-hr O<sub>3</sub> within a factor of 1.5, respectively. The recommended performance criteria for O<sub>3</sub> by U.S. EPA (1991) are: mean normalized bias  $\pm 5$  to  $\pm 15$ %; mean normalized gross error 30% to 35%; unpaired peak prediction accuracy:  $\pm 15$  to  $\pm 20$ %.

\* **Corresponding author address:** Shaocai Yu, E-43-01, NERL, U.S. EPA, RTP, NC 27711

The NMB and NME values for maximum 1-hr (maximum 8-hr) O<sub>3</sub> are 3.2% (9.0%) and 20.0% (21.8%), respectively, close to the performance criteria for the unpaired peak O<sub>3</sub>.

For the categorical evaluation, we calculated model Accuracy (A), Bias (B), Probability Of Detection (POD), False Alarm Rates (FAR) and Critical Success Index (CSI) based upon observed (exceedances, non-exceedances) versus forecasted (exceedance, non-exceedances) for both the maximum 1-hr and 8-hr standard (Table 1). The Accuracy of the model prediction, which indicates the percent of forecasts that correctly predict an exceedance or non-exceedance, is very high (97.9%). However, the CSI value, which provides a measure of how well the exceedances were predicted, are 11.7% and 35.8% for the maximum 1-hr and 8-hr exceedances, respectively, indicating poor performance on reproducing the observed exceedances.

### 3.2 Diagnostic evaluation during the 2002 NEAQS

Figure 2 presents an example of time-series comparisons and scatter plots of the model predictions and observations for O<sub>3</sub>, NO, NO<sub>2</sub>, CO, NO<sub>y</sub>, and PAN at the HF site. The model captured the hourly variations and broad synoptic-scale changes seen in the observations of different gas species (O<sub>3</sub>, NO<sub>2</sub>, CO, NO<sub>y</sub>, PAN, SO<sub>2</sub>) (correlation coefficient > 0.50, see Table 2) except NO at each site, although there were occasional major excursions. For the photolysis rates of NO<sub>2</sub>, we focus our analysis on daytime data by excluding data where  $JNO_2 < 5 \times 10^{-5} \text{ s}^{-1}$ . Table 2 indicates that the model reproduced 77.1%, 64% and 70.9% of observed JNO<sub>2</sub> values within a factor of 1.5 at the CS, MWO and TF sites, respectively. DeMore et al. (1997) suggest that a ±20% uncertainty was associated with uncertainty in the cross-section and quantum yield data in the calculation of JNO<sub>2</sub> values. The sensitivity tests of Hanna et al. (2001) indicate that a 50% uncertainty in NO<sub>2</sub> photolysis rate could cause about a 40 ppbv, or a 20% uncertainty in predicted maximum O<sub>3</sub> concentration in their cases. This suggests that priority should be given to more accurate determination of the JNO<sub>2</sub> values in the model to get good O<sub>3</sub> predictions, especially during the cloudy periods as cloud cover can significantly affect the JNO<sub>2</sub> values.

Comparisons of modeled and ship-based Lidar observed O<sub>3</sub> vertical profiles provide an assessment for the ability of the model to simulate

the vertical structure of air pollutants. Figure 3 indicates that while the model reproduced the observed vertical structure, it tended to overpredict in the higher layers.

The [O<sub>3</sub>]/[NO<sub>x</sub>] values can be used to determine NO<sub>x</sub>-sensitive and VOC-sensitive chemical regimes. Following Arnold et al. (2003), the total hours spent in each extreme region and nearer to the [O<sub>3</sub>] ridgeline according to the [O<sub>3</sub>]/[NO<sub>x</sub>] values are calculated and listed in Table 3 for the HF, CS and TF sites. [O<sub>3</sub>]/[NO<sub>x</sub>] values > 46 indicate strong NO<sub>x</sub>-sensitive conditions, whereas its values < 14 indicate VOC-sensitive conditions (Arnold et al., 2003). Table 3 reveals that for the most part, the model correctly reproduced the temporal variations in the observed [O<sub>3</sub>]/[NO<sub>x</sub>] ratios across the different conditions represented at the three sites.

The fraction of NO<sub>y</sub> converted to NO<sub>z</sub> can be used to represent the air mass photochemical age. It is found that the percentages of the daytime (6:00 to 18:00 EST) hours with air mass photochemical age values [NO<sub>z</sub>]/[NO<sub>y</sub>] > 0.6 for the model are 96%, 56% and 87% at the CS, TF and HF sites, respectively, in agreement with the observations of 82%, 72% and 82% at the CS, TF and HF sites, respectively. These results are similar to those reported by Olszyna et al. (1994).

The O<sub>3</sub>-CO correlations have been used to diagnose pollution influence of anthropogenic sources on O<sub>3</sub>. Following Chin et al. (1994), we only used the observed data with NO<sub>x</sub>/NO<sub>y</sub> < 0.3 (photochemically aged rural air) and obtained during the period from 13:00 to 17:00 LST. Strong correlations between O<sub>3</sub> and CO for both model predictions and observations with a consistent slope  $\partial O_3 / \partial CO$  indicate that the modeled lower limits of the ozone production efficiencies ( $\eta_N$ ) values are close to the observations at the AIRMAP and HF sites. The upper limits of  $\eta_N$  value can be estimated by the O<sub>3</sub>-NO<sub>z</sub> slope. Following Arnold et al. (2003), both modeled and observed O<sub>3</sub>-NO<sub>z</sub> slopes are obtained for only observational data with [O<sub>3</sub>]/[NO<sub>x</sub>] > 46 at the three sites. There is significant correlation between O<sub>3</sub> and NO<sub>z</sub> for both model predictions and observations ( $r > 0.77$ ) at the three sites (see Fig. 4). Both modeled and observed  $\eta_N$  values at the three sites are in the estimated ranges (5 to 10) of other investigators (Olszyna et al., 1994) at rural sites in the eastern US, although the modeled  $\eta_N$  values (4.3 to 5.1) are about half of the observations (8.3 to 10.0). The scatter plots of Figure 4 also show that the modeled NO<sub>z</sub> concentrations were higher than the observations, indicating that the model chemistry put more NO<sub>x</sub>

into terminal products (NO<sub>y</sub>) as opposed to O<sub>3</sub> than in real world.

#### 4.0 REFERENCES

Arnold, J.R., R.L. Dennis, and G.S. Tonnesen, 2003: Diagnostic evaluation of numerical air quality models with specialized ambient observations: testing the Community Multiscale Air Quality modeling system (CMAQ) at selected SOS 95 ground sites. *Atmospheric Environment*, 37, 1185-1198.

Byun, D.W. and J.K.S. Ching, Eds., 1999: Science algorithms of the EPA Models-3 Community Multi-scale Air Quality (CMAQ) modeling system, EPA/600/R-99/030, Office of Research and Development, U.S. Environmental Protection Agency.

Chin, M., D.J. Jacob, J.W. Munger, D.D. Parrish, and B.G. Doddridge, 1994: Relationship of ozone and carbon monoxide over North America, *Journal of Geophysical Research*, 99, 14565-14573.

DeMore, W.B., S.P. Sander, C.J. Howard, A.R. Ravishankara, D.M. Golden, C.E. Kolb, R.F. Hampson, M.J. Kurylo, and M.J. Molina, 1997: Chemical kinetics and photochemical data for use in stratospheric modeling, Eval. 12, NASA Jet Propul. Lab., Calif. Inst. Of Technol., Pasadena.

Hanna, S.R., Z. Lu, H.C. Frey, N. Wheeler, J. Vukovich, S. Arunachalam, M. Fernau, and D.A. Hansen, 2001: Uncertainties in predicted ozone concentrations due to input uncertainties for the UAM-V photochemical grid model applied to the July 1995 OTAG domain. *Atmospheric Environment*, 35, 891-903.

Olszyna, K.J., E.M. Bailey, R. Simonaitis, and J.F. Meagher, 1994: O<sub>3</sub> and NO<sub>y</sub> relationships at a rural site. *Journal of Geophysical Research*, 99, 14,557-14,563.

Rogers, E., T. Black, D. Deaven, G. DiMego, Q. Zhao, M. Baldwin, N. Junker, and Y. Lin. 1996: Changes to the operational "early" Eta Analysis/Forecast System at the National Centers for Environmental Prediction. *Wea. Forecasting*, 11, 391-413.

EPA, 1991. Guideline for regulatory application of the urban airshed model. USEPA Report No. EPA-450/4-91-013. U.S. EPA, Office of Air Quality Planning and Standards, Research Triangle Park, North Carolina.

Table 1. Operational evaluation on the basis of the AQS data over the northeastern US

Discrete Statistics					
	RMSE (ppb)	MB (ppb)	NMB (%)	NME (%)	R
Hourly	24.23	12.55	29.77	46.87	0.63
Max 1-hr	17.65	2.32	3.24	20.05	0.70
Max 8-hr	17.03	5.74	9.02	21.86	0.70
Categorical Statistics					
	A (%)	B	FAR (%)	CSI (%)	POD (%)
Max 1-hr	97.94	0.36	60.7	11.7	14.3
Max 8-hr	82.60	0.76	39.0	35.8	46.38

Table 2. Statistical summaries of the comparisons of the model results with the observations at the different sites during the 2002 NEAQS.

Parameters	<C>*				
	Obs	Model	r	% within a factor of 1.5**	% within a factor of 2**
<b>Castle Springs (N=288)</b>					
O <sub>3</sub>	42.94	55.21	0.695	58.7	86.5
NO	0.15	0.03	0.172	9.3	18.1
CO	166.31	137.96	0.724	86.5	99.0
NO <sub>y</sub>	2.91	4.15	0.800	46.5	76.7
SO <sub>2</sub>	1.29	2.46	0.751	23.4	44.7
JNO <sub>2</sub> (1/S)	4.37×10 <sup>3</sup>	4.40×10 <sup>3</sup>	0.971	77.1	91.4
Temperature (C)	24.61	23.59	0.962	99.0	100.0
RH (%)	53.22	51.23	0.843	98.6	100.0
Wind direction	221	264	0.212	76.7	85.1
Wind speed (m/s)	1.89	3.11	0.405	39.5	62.3
<b>Harvard forest (N=288)</b>					
O <sub>3</sub>	60.01	60.26	0.773	80.8	92.0
NO	0.16	0.09	0.467	36.8	55.6
NO <sub>2</sub>	1.85	1.97	0.443	38.4	60.5
CO	197.75	220.55	0.804	87.8	98.0
NO <sub>y</sub>	6.10	9.20	0.766	40.1	74.1
PAN	0.62	1.23	0.690	24.2	47.2
RH (%)	74.08	60.65	0.882	96.6	100.0
Wind direction	242	261	0.002	88.9	90.5
Wind speed (m/s)	1.82	2.63	0.590	45.8	67.2
<b>Isle of Schoals (N=288)</b>					
O <sub>3</sub>	56.33	69.00	0.733	65.3	86.1
CO	237.93	168.00	0.631	48.1	90.6
<b>Mount Washington (N=288)</b>					
O <sub>3</sub>	60.65	53.11	0.827	86.3	99.3
NO	0.24	0.02	0.066	12.4	23.2
CO	154.59	119.68	0.639	82.7	96.0
SO <sub>2</sub>	1.23	1.52	0.662	33.2	48.4
JNO <sub>2</sub> (1/s)	4.01×10 <sup>3</sup>	4.72×10 <sup>3</sup>	0.917	64.0	77.7
<b>Thompson Farm (N=288)</b>					
O <sub>3</sub>	44.39	56.74	0.819	59.0	76.0
NO	0.16	0.19	0.636	23.7	42.0
CO	203.46	194.24	0.550	80.5	92.7
NO <sub>y</sub>	4.60	9.51	0.505	25.1	51.6
SO <sub>2</sub>	1.94	7.64	0.028	13.8	18.5
JNO <sub>2</sub> (1/s)	4.32×10 <sup>3</sup>	4.24×10 <sup>3</sup>	0.944	70.9	86.3
Temperature (C)	24.09	24.40	0.942	100.0	100.0
RH (%)	64.26	55.38	0.834	92.0	100.0
Wind direction	231.07	229.13	0.452	87.2	95.5
Wind speed (m/s)	2.26	2.31	0.380	48.5	70.6

\* <C> is the mean concentration (ppb)

\*\* Percentages (%) are the percentages of the comparison points at which model results are within a factor of 1.5 and 2 of the observations. N is number of samples.

Table 3. Statistical summary of number of hours for response surface indicator ratios (O<sub>3</sub>/NO<sub>x</sub>) for model and observations at each sites during the period of August 6 to 17, 2002. The values in parentheses are the percentages (%).

O <sub>3</sub> /NO <sub>x</sub>	Harvard Forest		Castle Springs		Thompson Farm	
	Obs	Model	Obs	Model	Obs	Model
0-14	28 (21)	16 (12)	1 (1)	0 (0)	16 (13)	25 (21)
15-25	11 (8)	26 (20)	13 (11)	0 (0)	13 (11)	10 (8)
26-45	11 (8)	20 (15)	12 (11)	11 (10)	16 (13)	15 (13)
>46	83 (62)	71 (53)	88 (77)	103 (90)	75 (63)	70 (58)
Total hours	133 (100)	133 (100)	114 (100)	114 (100)	120 (100)	120 (100)

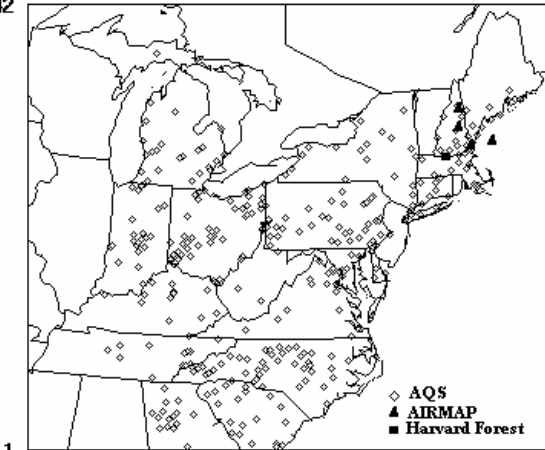


Fig. 1 The Eta-CMAQ model domain and locations of AQS, AIRMAP and Harvard Forest sites

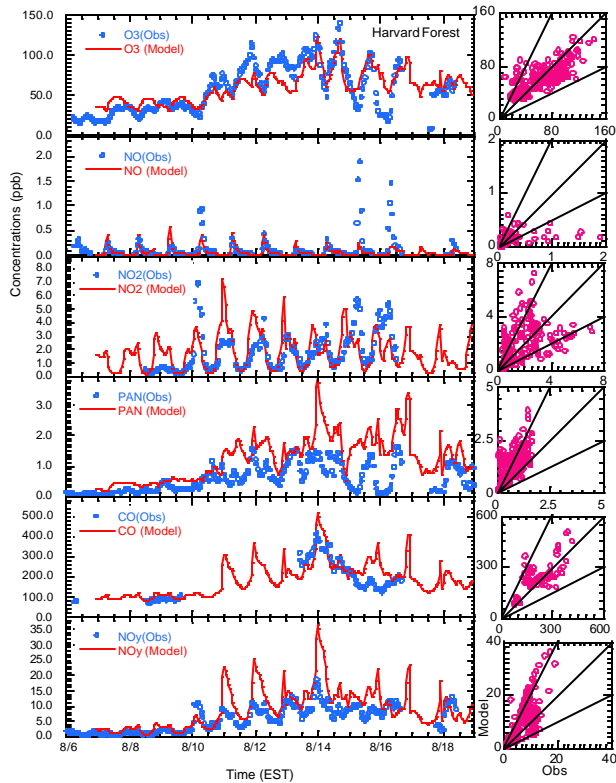


Fig. 2 Time-series and scatter plots of model predictions and observations at the Harvard Forest site

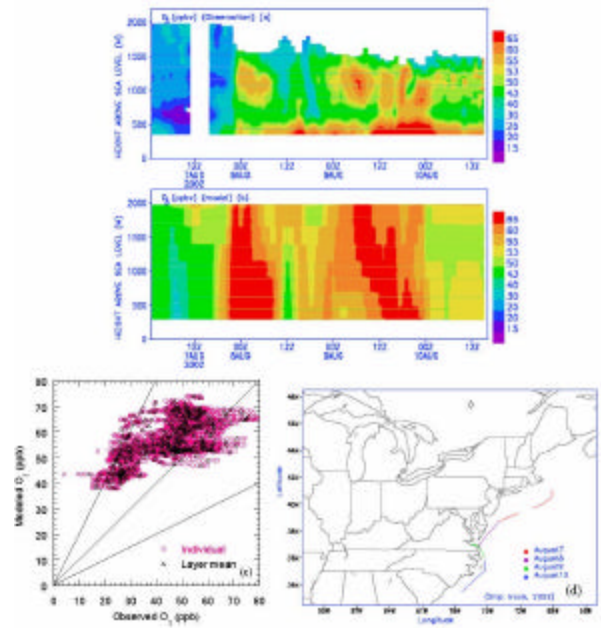


Fig. 3 Vertical O<sub>3</sub> profiles for the Lidar observations (a) and models (b) during the period from August 7 to 10, 2002. (c) scatter plots between the observations and model predictions for individual value and model-layer means and (d) ship tracks.

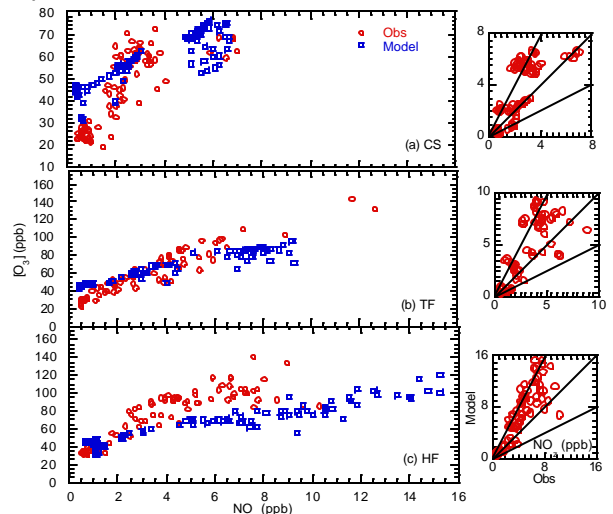


Fig. 4 O<sub>3</sub> as a function of NO<sub>z</sub> for the NO<sub>x</sub>-limited conditions indicated by the observational data with [O<sub>3</sub>]/[NO<sub>x</sub>] > 46 at (a) CS, (b) TF, and (c) HF. Right panels are scatter plots of modeled and observed NO<sub>z</sub>.

**Disclaimer** The research presented here was performed under the Memorandum of Understanding between the U.S. Environmental Protection Agency (EPA) and the U.S. Department of Commerce's National Oceanic and Atmospheric Administration (NOAA) and under agreement number DW13921548. Although it has been reviewed by EPA and NOAA and approved for publication, it does not necessarily reflect their policies or views.